Solid State Communications 251 (2017) 5–9

Contents lists available at ScienceDirect

Solid State Communications

journal homepage: www.elsevier.com/locate/ssc

Communication

Antiferromagnetic phase diagram of the cuprate superconductors

L.H.C.M. Nunes[b,*], A.W. Teixeira[b], E.C. Marino[a]

[a] Instituto de Física, Universidade Federal do Rio de Janeiro, Caixa Postal 68528, Rio de Janeiro, RJ 21941-972, Brazil
[b] Departamento de Ciências Naturais, Universidade Federal de São João del Rei, 36301-000 São João del Rei, MG, Brazil

ARTICLE INFO

Keywords:
High-Tc superconductors
Phase transitions

ABSTRACT

Taking the spin-fermion model as the starting point for describing the cuprate superconductors, we obtain an effective nonlinear sigma-field hamiltonian, which takes into account the effect of doping in the system. We obtain an expression for the spin-wave velocity as a function of the chemical potential. For appropriate values of the parameters we determine the antiferromagnetic phase diagram for the $YBa_2Cu_3O_{6+x}$ compound as a function of the dopant concentration in good agreement with the experimental data. Furthermore, our approach provides a unified description for the phase diagrams of the hole-doped and the electron doped compounds, which is consistent with the remarkable similarity between the phase diagrams of these compounds, since we have obtained the suppression of the antiferromagnetic phase as the modulus of the chemical potential increases. The aforementioned result then follows by considering positive values of the chemical potential related to the addition of holes to the system, while negative values correspond to the addition of electrons.

1. Introduction

Cuprates are puzzling materials; the undoped parent compounds are Mott insulators presenting an antiferromagnetic (AF) arrangement at a finite Néel temperature. As the system is doped, either with electron acceptors or donors, which, in any case would simply mean an increase of the amount of charge carriers to the system, it develops high-temperature superconductivity. The superconducting (SC) critical temperature presents a characteristic dome-shaped dependence on dopant concentration, reaching a maximum value at an optimal doping and vanishing as the system is doped even further, becoming a normal metal. So far, there is no consensus regarding the microscopic mechanism which is responsible for the appearance of superconductivity in those systems. However, it is widely accepted that some sort of AF spin fluctuations are the interaction responsible for the Cooper pairs formation.

Recently, starting from a spin-fermion model, which has been employed previously to describe the cuprate superconductors [1] we have derived an effective model for the charge carriers [2] and the superconductivity in our model arises from a novel mechanism, that yields a high critical temperature which is comparable to the experimental values. Moreover, by including doping effects a dome-shaped dependence of the critical temperature is found as charge carriers are added to the system, in agreement with the experimental phase diagram [3]. Presently instead of focusing on the SC phase, we investigate the magnetic order, by calculating the doping dependence of the Néel temperature, which is calculated providing the AF phase diagram that can be compared with experimental results. As shall be seen below, our results are in good agreement with the data for the $YBa_2Cu_3O_{6+x}$ (YBCO) system [4,5]. This calculation is an alternative to the one performed before [6], which was based on the fact that a skyrmion topological excitation is created in association to a doped charge, being actually attached to it.

Our approach provides a unified description for the phase diagrams of the hole-doped and the electron doped compounds, which is consistent with the experimental results [7]. As the dopant concentration increases, a dome-shaped SC phase appears adjacent to the AF order, both for electron-doped and hole-doped cuprate compounds as well. Our calculations present the suppression of the AF phase as the modulus of the chemical potential increases. Positive values of the chemical potential are related to the addition of holes to the system, while negative values correspond to the addition of electrons.

2. The spin-fermion model

So far, there is no consensus regarding the minimal model which entails the vast phenomenology presented by the high-T_c superconductors, however, since it is well established that superconductivity emerges from the CuO_2 planes of the cuprates, the paradigmatic three-band Hubbard model proposed by Emery [8] is a good candidate to describe the physics in these planes. However, due to its several parameters this model is a complicated starting model for the study

* Corresponding author.
E-mail addresses: lizardonunes@ufsj.edu.br (L.H.C.M. Nunes), marino@if.ufrj.br (E.C. Marino).

http://dx.doi.org/10.1016/j.ssc.2016.12.003
Received 2 August 2016; Received in revised form 2 December 2016; Accepted 6 December 2016
Available online 07 December 2016
0038-1098/

of the electronic properties in the CuO_2 planes. Therefore, many theoretical studies have considered instead a one-band Hubbard model or a single band *t-J* model [9] which represents the lower "Zhang-Rice singlet" [10] band of the original three-band Hubbard model. However, the approach that a simpler one-band Hubbard model or *t-J* models are capable of describing correctly the doped CuO_2 planes has been challenged recently [11] and we agree with this particular point of view that a strongly correlated single-band model cannot provide the appropriate description for the cuprates. Indeed, our starting point for the description of the CuO_2 planes is the spin-fermion model, which has been also extensively used to describe the high-T_c superconductors [1].

Henceforth, consider a single CuO_2 plane containing localized spins located at the sites of a square lattice, which is the appropriate topology for the cuprates. The spin degrees of freedom are modelled by the spin 1/2 AF Heisenberg model, $H_{\rm H} = J\sum_{<ij>}\mathbf{S}_i\cdot\mathbf{S}_j$, where $\mathbf{S}_i$ is the localized spin operator. As the system is doped, charge carriers are bumped into the planes and the localized spins interact with the spin degrees freedom of the itinerant fermionic charge carriers via a Kondo coupling, $H_{\rm K} = J_K\sum_i \mathbf{S}_i\cdot\mathbf{s}_i$, where $\mathbf{s}_i = \sum_{\alpha,\beta} c^\dagger_{i\alpha}\vec{\sigma}_{\alpha\beta}c_{i\beta}$ denotes the spin operator of an itinerant charge carrier, which is written in terms of the Pauli matrices $\vec{\sigma} = (\sigma_x, \sigma_y, \sigma_z)$ and $c^\dagger_{i\alpha}$ denotes the creation operator for a charge carrier at site i with spin $\alpha = \uparrow, \downarrow$. Combining the Heisenberg model, the Kondo coupling and the kinetic term associated to the itinerant charge carries, one obtain the spin-fermion model.

We formulate this model in the continuum limit, by employing the spin coherent states. This amounts to replacing the localized spin operators by $S\mathbf{N}(\mathbf{x})$, where S is the spin quantum number and $\mathbf{N}(\mathbf{x})$ is a classical vector such that $|\mathbf{N}(\mathbf{x})|^2 = 1$. $\mathbf{N}$ is then decomposed into two perpendicular components, $\mathbf{L}$ and $\mathbf{n}$ ($\mathbf{L}\cdot\mathbf{n} = 0$), associated respectively with ferromagnetic and antiferromagnetic fluctuations [12,13]. In the continuum limit, where the lattice spacing should be very small, $\mathbf{N}(\mathbf{x})$ is decomposed as $\mathbf{N}(\mathbf{x}) = a^2\mathbf{L}(\mathbf{x}) + (-1)^{|\mathbf{x}|}\mathbf{n}(\mathbf{x}) + O(a^4)$, where a denotes the lattice parameter and we also have $|\mathbf{n}(\mathbf{x})|^2 = 1$.

The continuum limit of the AF Heisenberg model in the square lattice is the well-known nonlinear sigma model (NLSM) [14], which is given by the following density Hamiltonian,

$$\mathcal{H}_{\rm H} = \frac{1}{2}(\rho_s|\nabla\mathbf{n}|^2 + \chi_\perp S^2|\mathbf{L}|^2) + iS\mathbf{L}\cdot(\mathbf{n}\times\partial_\tau\mathbf{n}), \tag{1}$$

where $\rho_s = JS^2$ is the spin stiffness, $\chi_\perp = 4Ja^2$ is the transverse susceptibility and the last term in the rhs of the above expression describes the Berry phase.

On the same token, the hamiltonian density of the Kondo interaction becomes

$$\mathcal{H}_{\rm K} = J_{\rm K}S\ \mathbf{L}\cdot\sum_{\alpha,\beta}\psi^\dagger_\alpha(\vec{\sigma})_{\alpha\beta}\psi_\beta, \tag{2}$$

where the continuum fermion field $\psi_\alpha(\mathbf{x})$ corresponds to $c_{i\alpha}$. Also notice that the oscillating contribution from the antiferromagnetic fluctuations cancels out as we integrate it over space [13].

For the cuprates, it is well known that Dirac points appear in the intersection of the nodes of the *d*-wave superconducting gap and the two-dimensional (2D) Fermi surface. In that case, the quasiparticles dispersion exhibit a Dirac-like linear energy dispersion [15]. Presently, we assume that the dispersion of the charge carriers can be linearized close to the Fermi surface and therefore the carrier kinematics in the continuum limit is described by the Dirac-Weyl density hamiltonian, as previously seen in [16],

$$\mathcal{H}_0 = \psi^\dagger(i\hbar v_F\vec{\sigma}\cdot\vec{\nabla} - \mu)\psi, \tag{3}$$

where $\psi^\dagger_\sigma$ has spinorial components $\psi^\dagger_\sigma = (\psi^\dagger_{1\sigma}, \psi^\dagger_{2\sigma})$ and v_F is the Fermi velocity. The indices 1 and 2 denote odd and even lattice sites respectively. Notice that the chemical potential μ controls the total number of charge carriers that are added to the itinerant band as the system is doped.

Hence, in the continuum limit we may express the partition function of the spin-fermion model as the following functional integral in the complex time representation

$$\mathcal{Z} = \int\mathcal{D}\psi\mathcal{D}\psi^\dagger\mathcal{D}\mathbf{L}\mathcal{D}\mathbf{n}\delta(|\mathbf{n}|^2 - 1)\times\exp\left[-\int_0^\beta d\tau\int d^2x(\mathcal{H} - \psi^\dagger i\partial_\tau\psi)\right], \tag{4}$$

where $\beta = 1/k_BT$, with k_B denoting the Boltzmann's constant and T the system temperature, and $\mathcal{H} = \mathcal{H}_{\rm H} + \mathcal{H}_{\rm K} + \mathcal{H}_0$, is given by (1), (2) and (3) respectively.

3. The effective nonlinear sigma model

We start by Fourier transforming our model Hamiltonian assuming that the ferromagnetic component of the vector spin $\mathbf{L}$ is small and approximately constant in space, since we investigate the system in the long range AF state ordering. Therefore, the Kondo interaction from (2) is approximated by

$$H_{\rm K} = J_{\rm K}S\int d^2k\int d^2k' \tag{5}$$

$$\times\sum_{\alpha,\beta}\psi^\dagger_\alpha(\mathbf{k})\left[\int d^2x\ e^{-i(\mathbf{k}-\mathbf{k}')\cdot\mathbf{x}}\mathbf{L}\right]\cdot(\vec{\sigma})_{\alpha\beta}\psi_\beta(\mathbf{k}')$$

$$\approx J_{\rm K}S\mathbf{L}\cdot\int d^2k\left[\sum_{\alpha,\beta}\psi^\dagger_\alpha(\mathbf{k})(\vec{\sigma})_{\alpha\beta}\psi_\beta(\mathbf{k})\right]. \tag{6}$$

In this approximation, we may introduce the Nambu field $\Phi^\dagger = (\psi^\dagger_{1,\uparrow}\psi^\dagger_{2,\uparrow}\psi^\dagger_{1,\downarrow}\psi^\dagger_{2,\downarrow})$ in order to express the fermionic part of our model Hamiltonian $\mathcal{H}_\psi \equiv \mathcal{H}_{\rm K} + \mathcal{H}_0 - \psi^\dagger i\partial_\tau\psi$ in momentum space, $\mathbf{p} = \hbar\mathbf{k}$, as $\mathcal{H}_\psi = \Phi^\dagger(\mathbf{k})\mathcal{A}\Phi(\mathbf{k})$, where the matrix $\mathcal{A}$ above is given by

$$\mathcal{A} = \begin{pmatrix}\tilde{\mu}_+ & k_- & L_- & 0\\ k_+ & \tilde{\mu}_+ & 0 & L_-\\ L_+ & 0 & \tilde{\mu}_- & k_-\\ 0 & L_+ & k_+ & \tilde{\mu}_-\end{pmatrix}, \tag{7}$$

with the following definitions in the above expression, $k_\pm = -\hbar v_F(k_x \pm ik_y)$, $\tilde{\mu}_\pm = -i\omega_n + \mu \pm J_KS\,L_z$ and $L_\pm = J_KS(L_x \pm iL_y)$.

We may now integrate exactly the fermionic contribution of the partition function in (4), which is a simple Gaussian path integral and, hence, proportional to $\det\mathcal{A}$. Therefore,

$$\ln\mathcal{Z}_\psi = \ln\left(\prod_{\mathbf{p},n}\det\mathcal{A}\right) = \int d^2k\sum_n\ln[(\hbar v_Fk)^2 - (\mu_- - i\omega_n)^2]$$
$$+\int d^2k\sum_n\ln[(\hbar v_Fk)^2 - (\mu_+ - i\omega_n)^2], \tag{8}$$

where $\mu_\pm = \mu \pm |J_K\mathbf{L}|$ and $\omega_n = (2n+1)\pi\beta^{-1}$ are the Matsubara frequencies for fermions. Performing the sum over ω_n and after some algebra we get

$$\ln\mathcal{Z}_\psi = \int d^2k\sum_{s=\pm1}\{\beta\hbar v_Fk + \ln[1 + e^{-\beta(\hbar v_Fk+\mu_s)}] + \ln[1 + e^{-\beta(\hbar v_Fk-\mu_s)}]\}, \tag{9}$$

which is the same result obtained for a noninteracting relativistic system with a Zeeman term applied to it (e.g. [17]), but presently with $|J_K\mathbf{L}|$ corresponding to an external "magnetic field". Furthermore, notice that (9) yields to the partition function of a free fermion system when $\mathbf{L}\to 0$, as should be expected.

Now, we can integrate the above expression over the first Brillouin zone in momentum space. Also, notice that the Fermi surface of the YBCO system has rotational symmetry around the point (π, π). Using translational invariance, we shift the momentum around this point, thereby simplifying the integration over the first Brillouin zone. Introducing the change of variable $y = a_Dk/\pi$, where a_D is the lattice

spacing between dopants, we get

$$\ln \mathcal{Z}_\psi = \frac{\pi}{3}\gamma + \frac{\pi}{2}\sum_{s=\pm 1}\int_0^1 dy\, y\{\ln(1+e^{-\gamma y}z_s)+\ln(1+e^{-\gamma y}z_s^{-1})\}, \tag{10}$$

where we have introduced the dimensionless parameters $\gamma = \beta\,\hbar v_F \pi/a_D$ and $z_s = e^{-\beta\mu_s}$, with $s = \pm 1$. Moreover, since we have assumed that $|\mathbf{L}|$ is small, we can expand $\mathcal{Z}_\psi$ as a Taylor series,

$$\mathcal{Z}_\psi = \exp[A(T,\mu) + B(T,\mu)|\mathbf{L}|^2 + O(|\mathbf{L}|^4)], \tag{11}$$

where the first factor in the rhs of the above expression, $\exp[A(T,\mu,\gamma)]$, does not contribute to the effective NLSM that will be obtained at the end of this section or to the calculation of the Néel temperature in the next section and hence shall be neglected. On the other hand, $B(T,\mu)$ seen in (11) is given by

$$B(T,\mu) = \frac{\pi}{2}\left(\frac{J_K S}{\gamma}\right)^2\left(\beta\gamma\left[1+\frac{\sinh(\beta\gamma)}{\cosh(\beta\gamma)+\cosh(\beta\mu)}\right]+\sum_{s=\pm 1}\{\ln(1+e^{s\beta\mu})+\ln[1+e^{\beta(\gamma+s\mu)}]\}\right). \tag{12}$$

Combining (12) and (1), the NLSM becomes

$$\widetilde{\mathcal{H}}_{\rm H} = \frac{1}{2}[\rho_s|\nabla\mathbf{n}|^2 + \widetilde{\chi}_\perp(T,\mu)|\mathbf{L}|^2] + iS\mathbf{L}\cdot(\mathbf{n}\times\partial_\tau\mathbf{n}), \tag{13}$$

where the above new transverse susceptibility $\widetilde{\chi}_\perp$ includes the effect of doping, since it depends on the chemical potential,

$$\widetilde{\chi}_\perp(T,\mu) = \chi_\perp S^2 - \frac{2}{\beta}B(\mu,T). \tag{14}$$

Inserting (14) in (4) and integrating over $\mathbf{L}$ we finally get the partition function, except for a multiplicative factor,

$$\mathcal{Z} = \int \mathcal{D}\mathbf{n}\,\delta(|\mathbf{n}|^2-1)\exp\left(-\int_0^\beta d\tau\int d^2x\,\widetilde{\mathcal{H}}_{\rm eff}\right), \tag{15}$$

where the effective NLSM is

$$\widetilde{\mathcal{H}}_{\rm eff} = \frac{\rho_s}{2}\left[|\nabla\mathbf{n}|^2 + \frac{1}{c(T,\mu)^2}|\partial_\tau\mathbf{n}|^2\right], \tag{16}$$

with the new spin wave velocity given by

$$c(T,\mu) = \sqrt{\rho_s\chi_\perp\left[1-8\frac{B(\mu,T)}{\beta\chi_\perp}\right]}. \tag{17}$$

Notice that c in the above expression reduces to $c = \sqrt{\rho_s\chi_\perp}$ in the absence of the Kondo coupling, as should be expected.

In the present approach the spin wave velocity is finite for $\mu = 0$, which is related to the parent compounds of the cuprates and it is an even function with respect to the chemical potential. Indeed, positive values of μ are related to hole-doped cuprate superconductors, while $\mu < 0$ corresponds to the electron-doped compounds. Notice that doped electrons enter the Cu sites for the electron-doped compounds, which is not the case for the hole-doped cuprates, where doping introduces carriers at the oxygen sites. However, in a continuum limit description there is no difference between holes moving on an otherwise inert O-lattice, in the presence of an AF background on the Cu sites and electrons moving on the Cu sites in the presence of the same AF background and an inert O-lattice. The only difference perhaps would be on the value of the exchange coupling.

4. Néel temperature calculation and comparison with experimental data

We start our analysis pointing out that the Coleman-Mermin-Wagner-Hohenberg theorem prevents the appearance of a long-range magnetic order at finite temperatures for any 2D system [18]. Therefore, we add an small out-of-plane interlayer coupling $J_\perp$, so that the partition function for a stack of CuO_2 planes labeled by the subscript i becomes

$$\mathcal{Z} = \prod_i\int\mathcal{D}\mathbf{n}_i\exp\left\{-\int_0^{\hbar\beta}d\tau\int d^2x\times\delta(|\mathbf{n}_i|^2-1)\left[\frac{\widetilde{\mathcal{H}}_{\rm eff}}{\hbar}+\frac{\rho_s\alpha}{\hbar}(\mathbf{n}_{i+1}-\mathbf{n}_i)^2\right]\right\}, \tag{18}$$

where we have introduced the parameter $\alpha = (1/a^2)J_\perp/J$.

Assuming that there is an external magnetic field applied to the system, one may calculate T_N with several approaches, among them spin-wave theories (SWT) and field-theoretical calculations, which takes into account the contribution of the spin-fluctuation excitations (neglected in the SWT). Both the standard and self-consistent SWT are shown to be insufficient to quantitatively describe the experimental data for the parent compounds of the cuprates superconductors, while the results calculated for a large N expansion are in good agreement with the experiments [19]. Hence, we take the expression for T_N obtained to order $1/N$ in a large N expansion from the effective model in (18), which is given by [20]

$$T_N = 4\pi\rho_s\left[\ln\left(\frac{2\,T_N^2}{\alpha(\hbar c')^2}\right)+3\ln\left(\frac{4\pi\rho_s}{T_N}\right)-0.0660\right]^{-1}, \tag{19}$$

where $c' = (a/\hbar)c$. Moreover, we have set $k_B = 1$ for the sake of simplicity. Notice that the above expression provides a self-consistent equation for the calculation of the Néel temperature as a function of the chemical potential, since the spin wave velocity c in (17) is expressed in terms of μ.

In the remaining of this section we compare the results of the Néel temperature as a function of doping with the available experimental data for YBCO. Indeed, this compound has an almost circular shape for the Fermi surface centered at (π,π) in the reciprocal space [21] and the low energy dispersion can be approximated to a linear relation in the vicinity of the Fermi level, which is consistent with the kinetic term given by (3).

In terms of the three-band Hubbard model parameters, the exchange coupling between the Cu magnetic moments is given by [22,23]

$$J = \frac{4t_{pd}^4}{(\Delta E+U_{pd})^2}\left(\frac{1}{U_d}+\frac{2}{2\Delta E+U_p}\right) \tag{20}$$

and the Kondo coupling of an itinerant oxygen hole spin and the nearest local Cu spin is [22,23]

$$J_k = t_{pd}^2\left(\frac{1}{\Delta E}+\frac{1}{U_d-\Delta E}\right). \tag{21}$$

Estimates for the microscopic parameters of the three-band model Hamiltonian have been obtained from local-density functional techniques [24]: $t_{pd} = 1.3$, $U_d = 7.3$, $U_p = 5$, $U_{pd} = 0.87$ and $\Delta E = 3.5$, all given in units of eV. Inserting the above parameters values in (19) yields $T_N \approx 420$ K for the undoped system ($\mu = 0$), which is in excellent agreement with the experimental data for YBCO, and therefore we employ those values in our numerical calculation from now own.

Fom (17), one can calculate the spin wave velocity as a function of the chemical potential numerically for a particular temperature, provided the values for ρ_s, $\chi_\perp$ and γ are given. In our case, these are calculated from J_K and J in (20) and (21), with the parameters values given above, and also $\hbar v_f = 1.15$ eVÅ, $a_D = 2.68$ Å and $a = \sqrt{2}\,a_D$ [6]. Our numerical results are shown in Fig. 1 for the particular value of $T = 420$ K. Notice that for the undoped parent compound, we assume that the Dirac point is at $\mu = 0$, which is exactly the case for the cuprates. As the chemical potential increases for positive values, which means that holes are added to the CuO_2 planes, c vanishes indicating the destruction of the long range AF order, what is in agreement with the experimental results. On the other hand, for negative values of μ,

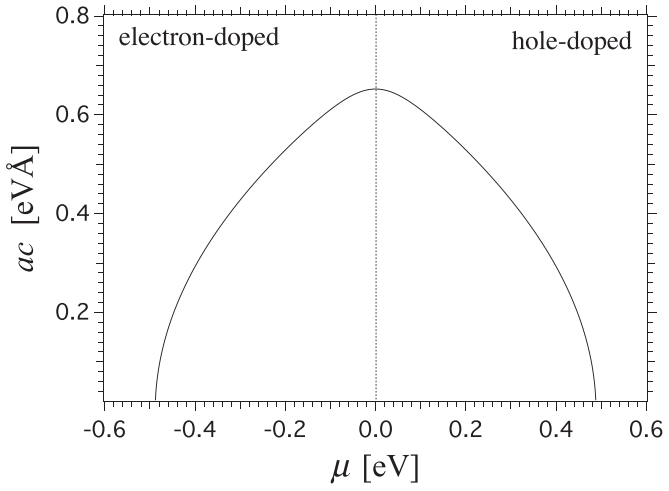

Fig. 1. Spin wave velocity multiplied by the lattice parameter ac as a function of the chemical potential μ for $T = 420$ K.

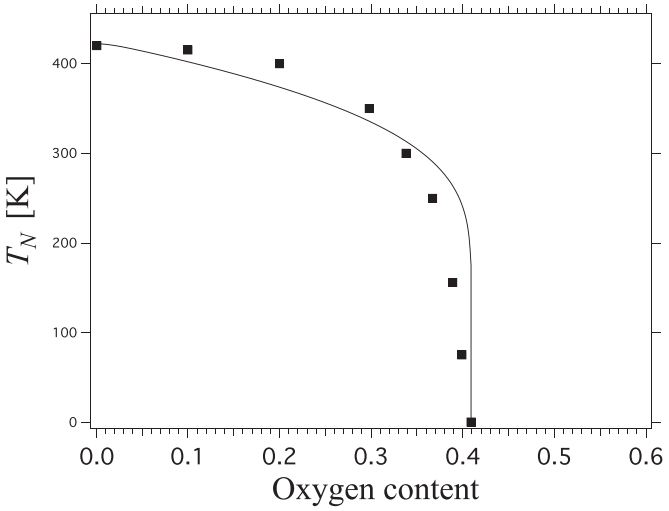

Fig. 2. Néel temperature T_N as a function of doping x for YBCO. Squares indicate experimental data from Ref. [5].

we also have that the spin wave velocity vanishes as μ increases in modulus, which corresponds to the doping of electrons, instead of holes, to the system. Therefore our approach provides a unified description for the phase diagrams of the p-type and n-type cuprate superconductors, where $\mu > 0$ are related to hole-doped systems, while $\mu < 0$ are electron-doped ones.

We can also calculate T_N as a function of the chemical potential from (19). It is well known that the occupancy of charge carriers increases as $\mu > 0$ also increases. Therefore, in order to compare our numerical results with the AF part of the phase diagram experimentally obtained for YBCO, we follow a phenomenological approach relating the chemical potential and the doping as $\mu - \mu_0 \propto (x - x_0)^\beta$, where μ_0 and x_0 are the chemical potential and the doping for which T_N reaches zero respectively. Since μ_0 is numerically calculated and x_0 is given by experiments, the proportionality constant is uniquely defined and β is the single parameter which has been adjusted to the available data. The results of the AF phase diagram for the YBCO parameters and $\beta \approx 3$ are shown in Fig. 2 and we see that our theory is in good agreement with the experiments [4,5]. Moreover, we also have that the magnetic order is suppressed as charge carriers are added to the system, as should be expected.

5. Conclusions

Starting from the spin-fermion model we have obtained an effective nonlinear sigma model which takes into account the effects of doping in the system. Taking the appropriate values of the parameters for YBCO, we have calculated the AF phase diagram as a function of the dopant concentration and the results presented here are in good agreement with the experimental data [4,5]. Notice that several studies indicate that there is a quantum phase transition as the ratio J/J_K increases, starting from a Fermi liquid state, the system becomes a spin liquid [25]. Presently, on the other hand, the interaction couplings are not model parameters, but provided by the experimental data available for the YBCO compound and henceforth it is remarkable that the system presents an AF arrangement in the absence of doping for the given values of J and J_K, which is in agreement with the phenomenology of the cuprates. Moreover, the calculated Néel temperature is consistent with the experimental data for T_N, since the results were obtained without resorting to any kind of parameter adjustment.

Recently, also starting from the spin-fermion model, we have obtained an effective interaction among the charge carriers of the system, which produces a dome-shaped SC high critical temperature versus doping [2] plot that qualitatively reproduces the SC phase diagram experimentally observed. Hence, combining our results, the following picture emerges: for the effective model of the localized spins presented here, where the itinerant fermions have been integrated out, we get the suppression of the magnetic order as charge carriers are added to the system; for the effective model of the itinerant fermionic fields, where the localized magnetic moments have been integrated out, we have the appearance of a dome-shape SC critical temperature with the addition of charge carriers [2]. Therefore, we have a theory where the AF order is suppressed and the SC phase arises as charge carriers added to the system, which is the phenomenology observed for several strongly correlated electronic systems [26]. However, the complete phenomenology of the cuprates, including its strange metal behavior in the underdoped regime remain unexplained [27].

Our results explain the qualitative similarities existing between hole and electron doped cuprates (positive and negative values of the chemical potential), however, they cannot account for the obvious quantitative differences between them. Among these, the most evident are the lower T_c and larger AF dome found in the latter. Hopefully, however, our study can provide a first step towards the understanding of the roles of electron and hole doping in high-T_c superconductivity. For this it would be essential to capture the differences produced by doping a hole into the O^{--} ions, in view of doping an electron into the Cu^{++}.

Further studies are therefore required in order to address the quantitative differences between the values for the T_c and T_N ordering temperatures of the cuprate compounds. At any instance, however, Dirac fields seem to play an important role in the physical properties of the cuprates [15].

Acknowledgements

E. C. Marino has been supported in part by the National Counsel of Technological and Scientific Development (CNPq) (Grant no. 307563/2015-4) and the Fundação de Amparo à Pesquisa do Estado do Rio de Janeiro (FAPERJ) (Grant no. E26/102975/2011).

References

[1] K.B. Efetov, H. Meier, C. Pépin, Nat. Phys. 9 (2013) 442;
E. Berg, E. Fradkin, S.A. Kivelson, Phys. Rev. Lett. 105 (2010) 146403;
Ar. Abanov, A. Chubukov, J. Schmalian, Adv. Phys. 52 (2003) 119;
M. Grilli, G.B. Kotliar, A.J. Millis, Phys. Rev. B 42 (1990) 329.
[2] E.C. Marino, L.H.C.M. Nunes, Ann. Phys. 340 (2014) 13.
[3] L.H.C.M. Nunes, A.W. Teixeira, E.C. Marino, Europhys. Lett. 110 (2015) 27008.
[4] D. Rybicki, M. Jurkutat, S. Reichardt, C. Kapusta, J. Hess, Nat. Commun. 7 (2016)

11413.
[5] J. Rossat-Mignod, et al., Physica B 169 (1991) 58.
[6] E.C. Marino, M.B.Silva. Neto, Phys. Rev. B 64 (2001) 092511.
[7] J.E. Hirsch, M.B. Maple, F. Marsiglio, Physica C. 514 (2015) 1 (and the references therein);
N.P. Armitage, P. Fournier, R.L. Greene, Rev. Mod. Phys. 82 (2010) 2421.
[8] V.J. Emery, G. Reiter, Phys. Rev. B 38 (1988) 4547;
V.J. Emery, Phys. Rev. Lett. 58 (1987) 2794.
[9] M. Ogata, H. Fukuyama, Rep. Prog. Phys. 71 (2008) 036501;
P.A. Lee, N. Nagaosa, X.-G. Wen, Rev. Mod. Phys. 78 (2006) 17.
[10] F.C. Zhang, T.M. Rice, Phys. Rev. B 37 (1988) 3759.
[11] C.P.J. Clemens, S. Moser, G.A. Sawatzky, M. Berciu, Phys. Rev. Lett. 116 (2016) 087002;
H. Ebrahimnejad, G.A. Sawatzky, M. Berciu, J. Phys.: Condens. Matter 28 (2016) 105603;
H. Ebrahimnejad, G.A. Sawatzky, M. Berciu, Nat. Phys. 10 (2014) 951.
[12] S. Sachdev, Quantum Phase Transitions, Cambridge University Press, Cambridge, UK, 1999.
[13] A. Tsvelik, Quantum Field Theory in Condensed Matter Physics, Cambridge University Press, Cambridge, UK, 1995.
[14] E. Manousakis, Rev. Mod. Phys. 63 (1991) 1.
[15] T.O. Wehling, A.M. Black-Schaffer, A.V. Balatsky, Adv. Phys. 76 (2014) 1.
[16] E.C. Marino, M.B.Silva. Neto, Phys. Rev. B 66 (2002) 224512 (and the references therein).
[17] H. Caldas, R.O. Ramos, Phys. Rev. B 80 (2009) 115428.
[18] N.D. Mermin, H. Wagner, Phys. Rev. Lett. 17 (1966) 1133;
P.C. Hohenberg, Phys. Rev. 158 (1967) 383;
S. Coleman, Commun. Math. Phys. 31 (1973) 259.
[19] A. Katanin, Y.V. Irkhin, Phys.-Uspekhii 50 (2007) 613.
[20] Y.V. Irkhin, A.A. Katanin, Phys. Rev. B 55 (1997) 12318.
[21] M.A. Hossain, et al., Nat. Phys. 4 (2008) 527.
[22] J. Zannem, A.M. Oles, Phys. Rev. B 37 (1988) 9423.
[23] A.P. Kampf, Phys. Rep. 249 (1994) 219.
[24] A.K. MacMahan, J.F. Annet, R.M. Martin, Phys. Rev. B 42 (1990) 6268.
[25] B.H. Bernhard, B. Coqblin, C. Lacroix, Phys. Rev. B 83 (2011) 214427;
I. Paul, C. Pépin, M.R. Norman, Phys. Rev. Lett. 98 (2007) 026402;
M. Burdin, Grilli, D.R. Grempel, Phys. Rev. B 67 (2003) 121104R;
Q. Si, S. Rabello, K. Ingersent, J.L. Smith, Nature 413 (2001) 804.
[26] D.J. Scalapino, Rev. Mod. Phys. 84 (2012) 1383.
[27] B. Keimer, et al., Nature 518 (2015) 179.